Medium Effects for Very Fast Electron Transfer Reactions at Electrodes: the $[Ru(NH_3)_6]^{3+/2+}$ System in Water

Martin Muzikář and W. Ronald Fawcett*

Department of Chemistry, University of California, Davis, California 95616

Received: August 23, 2005; In Final Form: October 12, 2005

The reduction kinetics of $[Ru(NH_3)_6]^{3+}$ was studied at Au(111) and Au(100) single-crystal ultramicroelectrodes in dilute perchloric acid electrolytes. Both heterogeneous rate constants and experimental transfer coefficients varied with the crystallographic orientation of the gold surface. The value of the heterogeneous rate constant at Au(111) was significantly larger than that at Au(100). The experimental transfer coefficients also increased but in the opposite order. Standard rate constants at both electrodes increased with an increase in electrolyte concentration. Using double-layer data obtained in 0.01 M $HClO_4$, it is shown that the true transfer coefficient for this reaction is 0.5 within experimental error. The effective charge on the reactant which has a nominal charge of +3 is close to +1. The latter result reflects the distribution of charge within the polyatomic reactant.

Introduction

According to electron transfer theory,[1] the Gibbs energy barrier for this fundamental process is determined by three factors, namely, the inner sphere reorganization energy, the outer sphere reorganization energy, and the work done to bring the reactant(s) to the reaction site. Very fast electron transfer reactions are usually those which have a very small inner sphere reorganization energy. Under these circumstances, the second and third factors become important in determining the rate constant. At electrodes, the third factor is usually called the double layer effect or the medium effect. It is the most difficult to estimate because it involves a model for the double layer and assumptions about the location of the reactant within it near the electrode.

This laboratory has been interested in studies of double-layer effects on simple electron-transfer reactions for some time.[2] Recent work has focused on the reduction of complex transition metal ions at single-crystal gold electrodes.[3−5] The reactions studied were slow and, therefore, could be investigated by well-known techniques, such as cyclic voltammetry. Reactions such as the reduction of $[Ru(NH_3)_6]^{3+}$ are so fast that it was difficult to obtain a reproducible standard rate constant 10 years ago;[6] however, the introduction of ultramicroelectrode techniques[7] has made it possible to investigate these reactions. This was followed by the fabrication of single-crystal ultramicroelectrodes,[8] at which electrode kinetics can be studied with consideration of double-layer effects. This experimental advance is important because it can provide the information needed to test the details of electron transfer theory[1] for very fast reactions.

Baranski et al.[9] showed that high-frequency ac admittance experiments provide an excellent method for studying the kinetics of very fast electron-transfer reactions. In earlier work,[10] we demonstrated that kinetic data could be obtained as a function of potential close to the standard potential and made a careful analysis of the precision of this technique. In the case of the reduction of $[Ru(NH_3)_6]^{3+}$, values of the standard rate constant and apparent transfer coefficient were obtained as functions of electrolyte concentration at a polycrystalline gold electrode. Since the double layer properties are not reproducible from one polycrystalline electrode to another, only a qualitative analysis of double-layer effects was made.

In the present paper, our study of the $[Ru(NH_3)_6]^{3+}$ system is extended to Au(111) and Au(100) single-crystal ultramicroelectrodes (SCUMEs) in dilute solutions of $HClO_4$. Kinetic data obtained as a function of electrode potential are presented in electrolyte solutions of three different concentrations. The double-layer effect is then analyzed using capacitance data obtained at each electrode.

Experimental Section

Reagents. All reagents were analytical grade and were used without further purification. Hexaaminoruthenium(III) chloride, sodium metasilicate, hydrochloric acid, and perchloric acid (70%, redistilled and 99.999% purity), were purchased from Aldrich Chemical Company (U.S.A.) and gold wires (99.99% purity), from Alfa Aesar, (U.S.A.). The electrolyte solutions were prepared with water from a Barnstead Nanopure water system and had a resistivity in the range 17.9−18.1 MΩ cm.

Electrolyte solutions were purged with argon (Praxair Inc., U.S.A.) before an experiment and kept under argon during the measurement.

Preparation of Au SCUMEs. The gold SCUMEs were grown in silicate gel formed at a low pH with HCl and $HAuCl_4$ as described in earlier work.[8] The resulting gel with a pH of 1 was formed in a small glass tube which had a gold wire sealed into its bottom. Gel formation followed after the evaporation of a small amount of water. The glass tube was covered by a glass cap in which the second gold electrode was mounted. Current was passed through the cell for several days using a 1.5-V battery with a 107-kΩ resistor in series with the cell.[8]

Chlorine formed at the anode in the gel reacts with the dissolved gold trichloride and forms a Au(I) complex, which eventually disproportionates further from the anode, giving rise to gold microcrystals in the vicinity. Microcrystals of the desired facet without visible steps (Figure 1) were selected under a microscope and used for the preparation of the SCUMEs. The

* To whom correspondence should be addressed. E-mail: wrfawcett@ucdavis.edu.

10.1021/jp054759e CCC: $33.50
Published on Web 01/26/2006

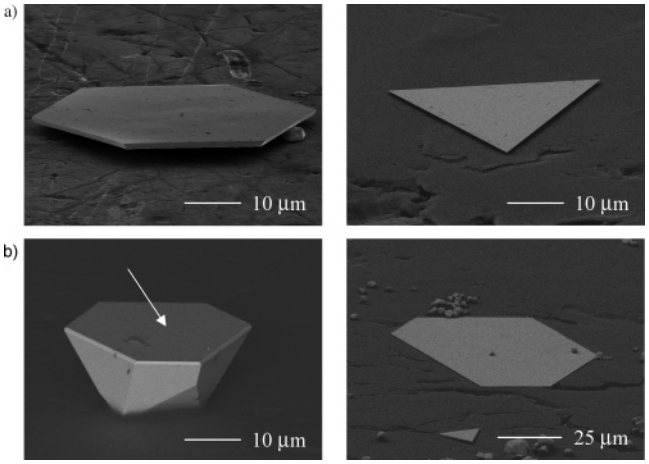

Figure 1. Scanning electron microscope images of single crystals (a) Au(111) and (b) Au(100).

microcrystal was soldered to a Au microwire and sealed into an inert epoxy so that only the desired facet was exposed to the electrolyte solution. Details regarding fabrication of the SCUMEs are given in earlier papers.[8,11]

Electrochemical Measurements. All electrochemical measurements were performed using a three-electrode system placed in a Pyrex glass cell with a Teflon cap. The cell was enclosed in a Faraday cage, which was connected to a common ground. Experiments were carried out at 25 ± 0.1 °C. The electrolyte solution was purged for 30 min with argon before electrochemical experiments and kept under an argon atmosphere during the experiments. Before each set of experiments, the SCUME was cycled for ~15 min in the perchloric acid electrolyte in a potential interval from −0.6 to 1.25 V versus a calomel electrode (0.05 M KCl) to clean the surface of the crystal. The reference electrode was connected to the electrolyte solution through a Luggin capillary. A gold wire of 1-mm diameter was used as the counter electrode.

Both cyclic voltammetry and ac admittance experiments were performed with an Autolab PG STAT30 potentiostat/galvanostat (ECO Chemie, The Netherlands) using a General-Purpose Electrochemical System plug-in (version 4.9) and frequency response analyzer software. The experimental setup was tested with an ac impedance dummy cell before starting the experiments.

Results

Cyclic voltammograms at SCUMEs in perchloric acid electrolytes have been recorded to confirm their single-crystal quality and crystallographic orientation. The current−voltage curves with characteristic shapes in the positive region have been obtained for Au(111) and Au(100) SCUMEs (see Figure 2). The shapes of the cyclic voltammograms were the same as those of gold standard size single-crystal electrodes[3] and clearly verified the single-crystal quality of the surfaces.

An important step in the analysis of the kinetic data is the precise determination of the electrode area. This has been accomplished by measuring the limiting current for reduction of the ferricyanide anion from voltammograms obtained under steady-state conditions. The area was estimated using the published diffusion coefficient for this process with 0.4 mM ferricyanide ion with 0.05 M KCl as the supporting electrolyte.[12] Once the effective area of the gold SCUMEs was known, this value was employed to calculate the rate constant from the faradic resistance for the electrode reaction.

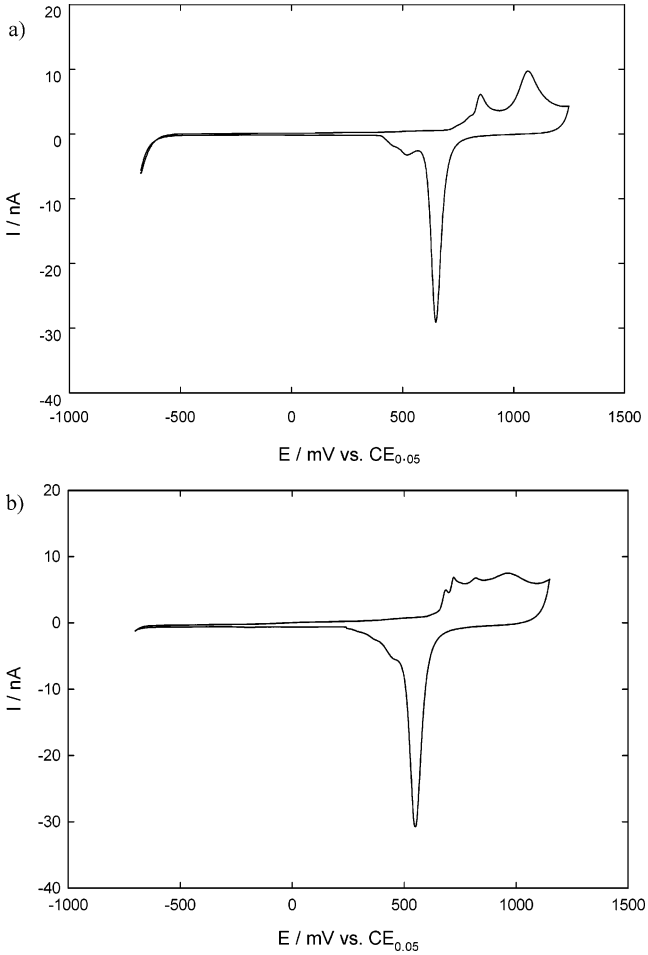

Figure 2. Cyclic voltammograms at (a) a Au(111) SCUME with an area of 8.2×10^{-5} cm^2 in 0.01 M $HClO_4$ at a scan rate of 50 mV s^{-1} and (b) a Au(100) SCUME with area of 7.5×10^{-5} cm^2 under the same conditions.

Kinetic Studies. Gold SCUMEs with an area on the order of 10^{-5} cm^{-2} were used in the experiments. The crystals were chosen with a shape as close as possible to a disk. For example, a hexagonal Au (111) crystal is a better choice than a triangular crystal (see Figure 1a). This is important insofar as mass transfer conditions are concerned. The Au(100) had the shape of a hexagon with alternate sides of unequal length, the ratio of the lengths being 1 to 1.5.

The crystals were insulated with a chemically resistant epoxy. To avoid possible adsorption of trace amounts of epoxy on the working surface of the gold microcrystals, the electrode was cycled before each set of experiments for ~20 min to clean the surface. The stability of the limiting current of the SCUME with time was carefully investigated. It was found that within the 2 h after the cleaning process, the current passing through the electrode remains stable, and adsorpion of epoxy did not occur. If the electrode was left overnight in the working solution, adsorption of epoxy on the SCUME surface was noted.

The kinetic data were obtained using high-frequency ac admittance voltammetry. Admittance versus potential plots were collected for different frequencies (usually in the range of 7−25 kHz) over the potential range of the faradic process. Typical data for the real and imaginary parts of the admittance as a function of potential are presented in Figure 3. The optimum frequency was chosen in a region where the faradic admittance was approximately equal to the double-layer admittance.

Determination of the heterogeneous rate constant was based on the Randles equivalent circuit for the interface in the presence

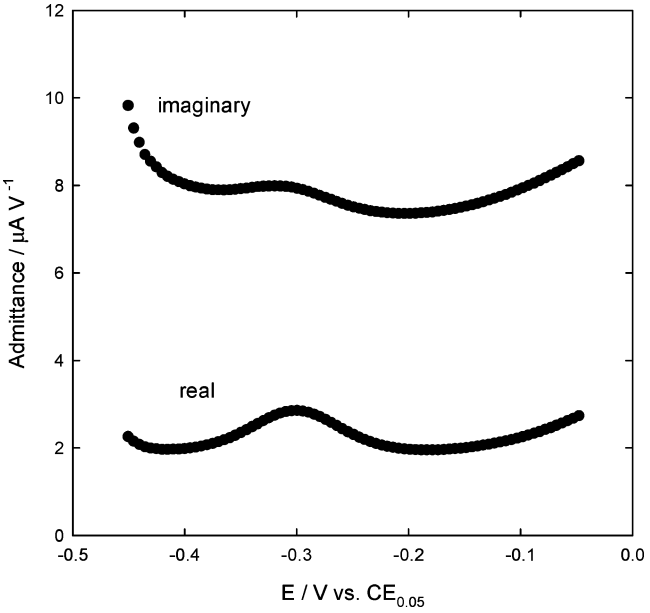

Figure 3. Admittance curves (ac) obtained for a Au(100) SCUME (area 1.38×10^{-5} cm^2) in a 0.02 M $HClO_4$ solution containing 0.5 mM $[Ru(NH_3)_6]^{3+}$; the ac frequency was 12 000 Hz.

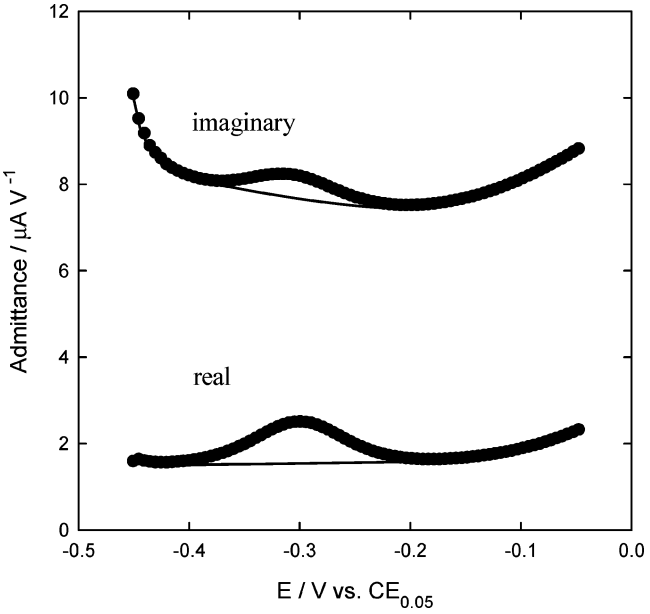

Figure 4. Admittance curves (ac) shown in Figure 3 after correction for the solution resistance.

of the reaction and was described in detail in our previous paper.[10] The solution resistance, R_s, and double-layer capacitance, C_{dl}, obtained in the absence of the faradic process were subtracted from the total admittance to obtain the faradic impedance for the region. In aqueous solutions, the solution resistance is small and does not significantly influence the kinetic data. After subtraction of the solution resistance, the real component of the admittance decreases slightly, and the imaginary component increases slightly (Figure 4).

To subtract the double-layer capacitance by a graphical method, the nonfaradic real and imaginary parts of the admittance in regions away from the faradic peak were fitted to a polynomial by least squares, and then a polynomial expression was used to evaluate the nonfaradic double-layer admittance and subtract it. The remaining admittance data provided information for calculation of the kinetic parameters.

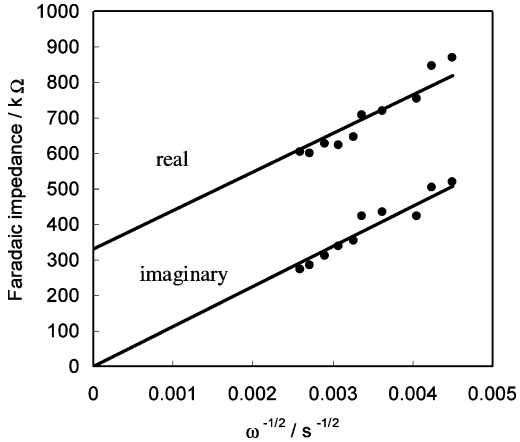

Figure 5. Randles plot of faradic admittance data for the reduction of 0.5 mM $[Ru(NH_3)_6]^{3+}$ at a Au(100) SCUME in 0.02 M $HClO_4$. The frequency range was 8−23 kHz. The value of R_{ct} estimated from this plot is 335 kΩ.

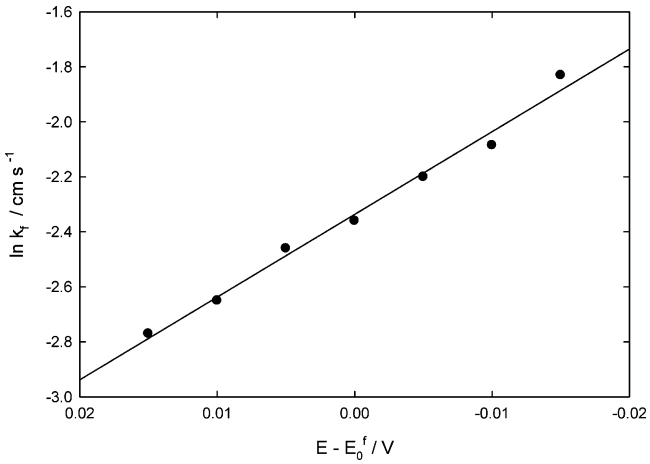

Figure 6. Baranski plot of data for the reduction of 0.5 mM $[Ru(NH_3)_6]^{3+}$ at a Au(100) SCUME in 0.02 M $HClO_4$. The ac frequency was 12 000 Hz.

The kinetic data were analyzed by two methods, as described previously.[10] According to the Randles analysis, the rate constant at a constant potential is obtained using admittance data obtained at several frequencies. This analysis was always carried out at the standard potential. In the Baranski analysis,[9] kinetic data at one frequency are analyzed as a function of potential. Typical data analyzed by the Randles method are shown in Figure 5. Both the real and imaginary parts of the faradic impedance depend linearly on the reciprocal of the square root of the angular frequency. The intercept of the real part of faradic impedance indicates the value of charge-transfer resistance, R_{ct}, from which the heterogeneous rate constant is calculated,

$$R_{ct} = \frac{RT}{n^2F^2Ac_A k_f} \tag{1}$$

where n is the number of electrons transferred (in this case, one electron); A, the area of the electrode; k_f, the forward rate constant; and c_A, the concentration of the reactant.

The Baranski method results in a plot of the rate constant as a function of potential for a given frequency (Figure 6). The rate constant and the experimental electron-transfer coefficient are calculated from the intercept and the slope of the resulting linear plot.

Experimental results in this study with estimates of errors are summarized in Table 1. Very good agreement between the

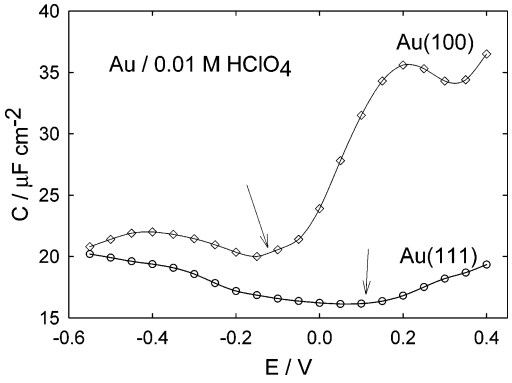

Figure 7. Plot of the interfacial capacitance as a function of potential. The arrows indicate the pzc at the two single crystals.

TABLE 1: Summary of Kinetic Data

solution	Randles k_s/cm s^{-1}	Baranski k_s/cm s^{-1}	Baranski α_{ex}	pzc/V vs $CE_{0.05}$
		Au(111)		
0.01 M $HClO_4$	0.30	0.31 ± 0.03	0.60 ± 0.04	0.150
0.02 M $HClO_4$	0.51	0.46 ± 0.04	0.56 ± 0.03	
0.03 M $HClO_4$	0.59	0.55 ± 0.04	0.54 ± 0.03	
		Au(100)		
0.01 M $HClO_4$	0.09	0.07 ± 0.02	0.76 ± 0.04	−0.160
0.02 M $HClO_4$	0.12	0.11 ± 0.02	0.71 ± 0.04	
0.03 M $HClO_4$	0.13	0.13 ± 0.03	0.69 ± 0.03	

standard rate constants from the Randles and Baranski analyses was obtained.

Double-Layer Data. The capacitance of the electrode≅olution interface was measured from the admittance of the system in the absence of the reactant. Then the specific capacity, C, was calculated using the area of the electrode. Capacity data obtained for the Au(111) and Au(100) interfaces in 0.01 M $HClO_4$ are shown in Figure 7.

Then the point of zero charge (pzc) was determined on the basis of the capacity minimum observed in solutions of lower ionic strength. On the present reference electrode scale, these are found at 0.150 V for the Au(111) electrode and at −0.150 V for the Au(100) electrode. It is then a simple matter to integrate the capacity data on a spreadsheet to obtain the electrode charge density σ_m. The potential drop across the diffuse layer ϕ^d can now be estimated using Gouy−Chapman theory:

$$\phi^d = \frac{2RT}{F}\ln\left(\frac{\sigma_m}{2A_{GC}} + \left(\frac{\sigma_m^2}{4A_{GC}^2} + 1\right)^{1/2}\right) \qquad (2)$$

A_{GC} is the Gouy−Chapman constant, which is equal to $5.8687c_e^{1/2}$ μC cm^{-2} in a solution whose aqueous concentration is c_e at 25 °C. As is well-known, ϕ^d increases in magnitude with σ_m and decreases with c_e.

Values of ϕ^d estimated at Au(111) and Au(100) for 0.01 M $HClO_4$ in the vicinity of the standard potential are shown in Figure 8. This potential region is negative of the pzc so that ϕ^d is negative at both electrodes. This corresponds to an accelerating effect for the positively charged reactant. Since ϕ^d is more negative at Au(111), the standard rate constant observed at this electrode is higher than at Au(100). However, as electrolyte concentration increases, the standard rate constants also increase. This result is more difficult to rationalize because the increase in electrolyte concentration should lead to a decrease in the magnitude of ϕ^d. This observation is discussed further below.

The other double-layer properties that are easily determined are the diffuse layer capacity, C_d, and the inner layer capacity,

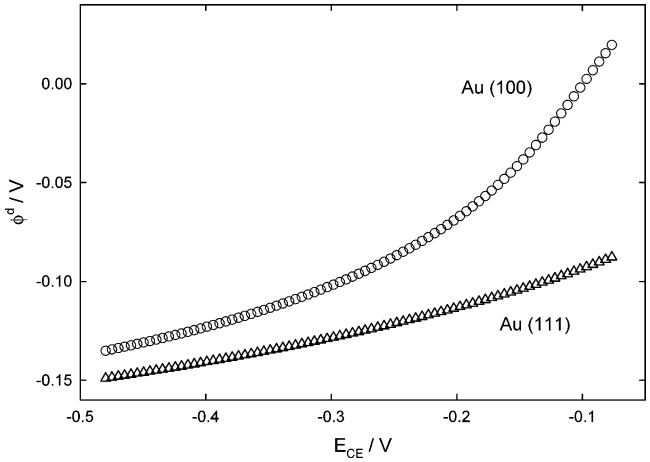

Figure 8. Plot of the potential drop across the diffuse layer ϕ^d for Au(111) and Au(100) against the electrode potential E_{CE} in the vicinity of the standard potential for reduction of $[Ru(NH_3)_6]^{3+}$ (−0.28 V).

C_{in}. The diffuse layer capacity for a given charge density and electrolyte concentration is given by

$$C_d = \frac{FA_{GC}}{RT}\left(\frac{\sigma_m^2}{4A_{GC}^2} + 1\right)^{1/2} \qquad (3)$$

Using this result and the differential capacity, C, one may calculate the inner layer capacity, C_{in}.

$$C_{in} = \frac{CC_d}{(C_d - C)} \qquad (4)$$

These quantities allow one to calculate important coefficients needed to analyze the double-layer effect. For example,

$$\frac{dE_{CE}}{d(E_{CE} - \phi^d)} = \frac{C_{in}}{C} \qquad (5)$$

and

$$\frac{d\phi^d}{d(E_{CE} - \phi^d)} = \frac{C_{in}}{C_d} \qquad (6)$$

In these equations, E_{CE} is the potential of the working electrode on the experimental potential scale, which uses a calomel electrode.

Analysis of the Double-Layer Effect. The expression giving the potential dependence of the forward rate constant is

$$\ln k_f = \ln k_{f0} + (\alpha - z_{ef})f\phi^d - \alpha f E_{CE} \qquad (7)$$

where k_{f0} is the value of the forward rate constant when both E_{CE} and ϕ^d are 0; z_{ef}, the effective charge on the reactant; α, the true value of the transfer coefficient; and $f = F/RT$. If the double-layer effect is ignored and the dependence of $\ln k_f$ on the electrode potential is determined, one obtains the experimental transfer coefficient, α_{ex}.

Thus,

$$-\frac{RT}{F}\frac{d\ln k_f}{dE_{CE}} = \alpha_{ex} = \alpha + (z_{ef} - \alpha)\frac{d\phi^d}{dE_{CE}} \qquad (8)$$

It follows that the experimental transfer coefficient is expected to be greater than the true transfer coefficient if the effective

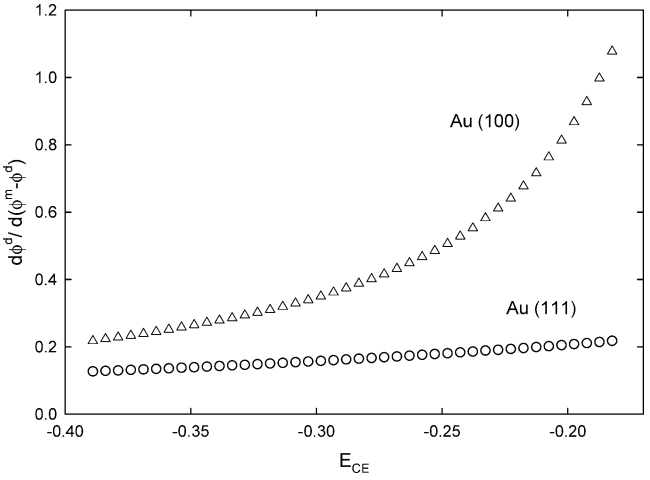

Figure 9. Plot of the coefficient $d\phi^d/d(E_{CE}-\phi^d)$ at Au(111) and Au(100) against the electrode potential E_{CE} in the vicinity of the standard potential for the reduction of $[Ru(NH_3)_6]^{3+}$ (−0.28 V).

TABLE 2: Double-Layer Data at the Standard Potential for the Reduction of $[Ru(NH_3)_6]^{3+}$ (−0.28 V) in 0.01 M $HClO_4$

electrode	σ_m $\mu C\ cm^{-2}$	ϕ^d V	C $\mu F\ cm^{-2}$	C_d $\mu F\ cm^{-2}$	C_{in} $\mu F\ cm^{-2}$
Au(111)	−7.2	−0.129	18.8	141.5	21.1
Au(100)	−2.5	−0.077	21.3	53.5	35.3

charge of the reactant is positive and greater than the true transfer coefficient α. The latter quantity is expected to be 0.5 for a simple electron-transfer reaction.[1] A problem with eq 8 is that the dependence of α_{ex} on α and z_{ef} is not separated; both the slope and intercept depending on α.

Thus, it is more convenient to define the apparent transfer coefficient on the basis of the following equation:

$$-\frac{RT}{F}\frac{d\ln k_f}{d(E_{CE}-\phi^d)} = \alpha_a = \alpha + z_{ef}\frac{d\phi^d}{d(E_{CE}-\phi^d)} \qquad (9)$$

On the basis of eqs 5 and 6, one may now write

$$\alpha_a = \alpha_{ex}\frac{C_{in}}{C} = \alpha + z_{ef}\frac{C_{in}}{C_d} \qquad (10)$$

If one can determine α_a and C_{in}/C_d at the two different SCUMEs, then one can estimate α and z_{ef} separately. For example, the coefficient $d\phi^d/d(E_{CE}-\phi^d)$ is quite different on Au(100) and Au(111), as shown in Figure 9. Since this coefficient is larger on Au(100), the experimental transfer coefficient is also larger (see Table 1).

Values of the double-layer parameters estimated at the standard potential for the $[Ru(NH_3)_6]^{3+}$ reaction in 0.01 M $HClO_4$ are summarized in Table 2. Using these data, the estimates of the apparent transfer coefficient at Au(111) is 0.69 and at Au(100), 1.26.

The corresponding values of C_{in}/C_d are 0.15 at Au(111) and 0.66 at Au(100). Using eq 10 and solving for the true transfer coefficient and effective charge, one obtains for α, 0.52, and for z_{ef}, 1.1. First of all, the value of α is 0.5 within experimental error. This is precisely the expected result for a simple electron-transfer reaction[1]. On the other hand, the effective charge on the reactant is considerably smaller than the formal charge (3+). Recent calculations by Nazmutdinov et al.[13] have shown that the effective charge on $[Ru(NH_3)_6]^{3+}$ is approximately the same as that on $[Co(NH_3)_6]^{3+}$ when these reactants are present at their distance of closest approach to a positively charged electrode. The experimental value of z_{ef} for $[Co(NH_3)_6]^{3+}$ is 2+[3]. The fact that z_{ef} is significantly smaller for $[Ru(NH_3)_6]^{3+}$ may be due to the fact that it reacts at a negatively charged electrode. Certainly, further study of the double layer effect for this system would be helpful in understanding why the effective charge is so low.

Discussion

On the basis of the data obtained at 0.01 M $HClO_4$, the reduction of the reactant occurs at negatively charged Au SCUMEs at a potential close to the pzc. If the charge on the electrode remains approximately constant at the standard potential when the electrolyte concentration is increased, then the standard rate constant should decrease due to a corresponding decrease in the potential drop across the diffuse layer, ϕ^d. In fact, the standard rate constant increases. This could be due to a shift in the electrode charge density to larger negative values. Unfortunately, double-layer data were not obtained at the higher concentrations so that the kinetic data cannot be analyzed further. This point certainly merits further investigation.

The striking result of the present study is that the effective charge on $[Ru(NH_3)_6]^{3+}$ is close to 1+. This means that the medium effect is much smaller than it would be if the effective charge were equal to the nominal charge of 3+. It also helps emphasize the importance of considering charge distribution effects in analyzing the effect of the double layer.[14,15] Charge distribution effects are also expected to be important in medium effects on homogeneous electron-transfer reactions.

Finally, the present study has shown that high-quality kinetic data may be obtained for very fast electron-transfer reactions. The availability of SCUMEs with two different orientations of gold provides a significant advantage in unraveling the details of the medium effect. We intend to extend our study to other very fast systems in both aqueous and nonaqueous media in an effort to elucidate the medium effect further.

Acknowledgment. This research was supported by a grant from the National Science Foundation, Washington (CHE-0133758 and CHE-0451103).

References and Notes

(1) Marcus, R. A. *J. Chem. Phys.* **1965**, *43*, 679.
(2) Fawcett, W. R. In *Electrocatalysis*; Lipkowski, J., Ross, P. N., Eds.; Wiley-VCH: New York, 1998; p 323.
(3) Hromadova, M.; Fawcett, W. R. *J. Phys. Chem. A* **2000**, *104*, 4356.
(4) Hromadova, M.; Fawcett, W. R. *J. Phys. Chem. A* **2001**, *105*, 104.
(5) Hromadova, M.; Fawcett, W. R. *J. Phys. Chem. B* **2004**, *108*, 3281.
(6) Fawcett, W. R.; Opallo, M. *Angew. Chem., Int. Ed. Engl.* **1994**, *33*, 2131.
(7) Fleischmann, M.; Pons, S.; Rolison, D. R.; Schmidt, P. *Ultramicroelectrodes*; Datatech Systems: Morganton, NC, 1987.
(8) Komanicky, V.; Fawcett, W. R. *Angew. Chem. Int. Ed.* **2001**, *40*, 563.
(9) Baranski, A. S. *J. Electroanal. Chem.* **1991**, *300*, 309.
(10) Muzikář, M.; Fawcett, W. R. *Anal. Chem.* **2004**, *76*, 3607.
(11) Komanicky, V.; Fawcett, W. R. *Electrochim. Acta* **2004**, *49*, 1185.
(12) Adams, R. N. *Electrochemistry at Solid Electrodes*; Marcel Dekker: New York, 1969; p 219.
(13) Nazmutdinov, R. R.; Rusanova, M. Yu.; Tsirlina, G. A. Unpublished results.
(14) Fawcett, W. R.; Hromadova, M.; Tsirlina, G. A.; Nazmutdinov, R. R. *J. Electroanal. Chem.* **2001**, *498*, 93.
(15) Rusanova, M. Yu.; Tsirlina, G. A.; Nazmutdinov, R. R.; Fawcett, W. R. *J. Phys. Chem. B* **2005**, *109*, 1348.